JPNT 7(3), 155-163 (2018)
https://doi.org/10.11003/JPNT.2018.7.3.155

JPNT Journal of Positioning, Navigation, and Timing

Performance Enhancement and Countermeasure for GPS Failure of GPS/INS Navigation System of UAV Through Integration of 3D Magnetic Vector

Heekwon No, Junesol Song, Jungbeom Kim, Yonghwan Bae, Changdon Kee†
Mechanical and Aerospace Engineering and SNU-IAMD, Seoul National University, Seoul 08826, Korea

ABSTRACT

This study examined methods to enhance navigation performance and reduce the divergence of navigation solutions that may occur in the event of global positioning system (GPS) failure by integrating the GPS/inertial navigation system (INS) with the three-dimensional (3D) magnetic vector measurements of a magnetometer. A magnetic heading aiding method that employs a magnetometer has been widely used to enhance the heading performance in low-cost GPS/INS navigation systems with insufficient observability. However, in the case of GPS failure, wrong heading information may further accelerate the divergence of the navigation solution. In this study, a method of integrating the 3D magnetic vector measurements of a magnetometer is proposed as a countermeasure for the case where the GPS fails. As the proposed method does not require attitude information for integration unlike the existing magnetic heading aiding method, it is applicable even in case of GPS failure. In addition, the existing magnetic heading aiding method utilizes only one-dimensional information in the heading direction, whereas the proposed method uses the two-dimensional attitude information of the magnetic vector, thus improving the observability of the system. To confirm the effect of the proposed method, simulation was performed for the normal operation and failure situation of GPS. The result confirmed that the proposed method improved the accuracy of the navigation solution and reduced the divergence speed of the navigation solution in the case of GPS failure, as compared with that of the existing method.

Keywords: magnetometer, unmanned aerial vehicle (UAV), global positioning system (GPS), inertial navigation system (INS)

1. INTRODUCTION

A global positioning system (GPS)/inertial navigation system (INS) integrated navigation system provides navigation solutions with a high output rate and accuracy using the complementary characteristics of inertial and satellite navigations. However, when it is impossible to use GPS, INS solely performs the navigation and the error of the navigation solution increases gradually. Although the failure of a GPS is rare because of the accumulated operational expertise; it is necessary to design a solution because GPS may be exposed to intentional jamming.

GPS/INS integrated navigation systems that use low-cost sensors exhibit insufficient observability for azimuth (Bar-Itzhack & Porat 1980, Rhee et al. 2004). A magnetometer is usually used to supplement these systems. As the heading calculated from the magnetic vector measured using the magnetometer can supplement GPS/INS navigation systems, low-cost GPS/INS navigation systems are generally integrated with a magnetometer. The attitude information of the roll and pitch angles is required to calculate the heading from the measured magnetic vector. When it is impossible to use GPS, the roll and pitch angles diverge, leading to inaccurate heading calculation results. The integration of such inaccurate heading with navigation systems may degrade navigation performance. Therefore, an alternative is required.

As a 3D vector shape, the geomagnetic field has the

Received Feb 22, 2018 **Revised** Jun 18, 2018 **Accepted** July 12, 2018
†**Corresponding Author**
E-mail: kee@snu.ac.kr
Tel: +82-2-880-1912 Fax: +82-2-888-2069

attitude information of two axes perpendicular to the vector direction. The integration of the 3D magnetic vector with GPS/INS navigation systems can improve the observability of the systems by providing additional attitude information besides the heading. Studies on estimating the attitude using the 3D magnetic vector integrated with GPS (Gebre-Egziabher & Elkaim 2008) and with GPS/INS navigation systems (Barczyk & Lynch 2012) exist, and in these studies, attitude accuracy was enhanced through improved observability. Moreover, the magnetic vector aiding method provides significant benefits when it is impossible to use GPS. First, this method does not require existing attitude information, unlike the magnetic heading aiding method; therefore, it is possible to use the method continuously even when GPS cannot be used. Second, when the observability of the system is enhanced by the aiding of the magnetic vector, the attitude accuracy and the related estimation accuracy of the inertial sensor error are also improved. This can considerably reduce the error accumulation of the navigation solution when INS solely performs navigation owing to a failure of GPS.

This paper proposes a countermeasure against performance degradation, which may occur in the case of GPS failure, by integrating the 3D magnetic vector to the GPS/INS integrated navigation system. The enhancement in the performance of the navigation system by improving observability is analyzed by comparing the results of the magnetic heading aiding method with the 3D magnetic vector aiding method. The effect of the magnetic vector aiding method is examined by performing simulations for the normal operation and for the failure situation of GPS; the proposed method is compared with the existing method.

2. GPS/INS INTEGRATED NAVIGATION

Most low-cost unmanned aerial vehicles (UAVs) use the highly cost-effective GPS/INS integrated navigation system. While the navigation solution of GPS based on a pseudorange has stable characteristics with the error not diverging over time, its noise level is high, and the output rate is low. The navigation solution of INS has a low noise level and high output rate; however, it diverges over time as the errors of inertial sensor measurements are accumulated. The GPS/INS integrated navigation system, which integrates the two navigation systems with complementary characteristics, can produce a navigation solution with low noise and high output rate in a stable manner. The GPS/INS integrated navigation is implemented through an extended Kalman filter. The error equation of INS is used as the system model, and the measurement model varies depending on the measurements of the GPS used. This study deals with the 17th order tightly coupled GPS/INS integrated navigation system including the GPS receiver clock error model, which uses the 15th order error equation suitable for UAVs performing 3D maneuvers as the system model, and by using the pseudorange and Doppler measurement model of the GPS receiver. The 17th order error equation is

$$\delta x = F \cdot \delta x + \Gamma w \tag{1}$$

where

$$\delta x = \begin{bmatrix} \delta p & \delta v & \delta \varepsilon & \delta b_a^b & \delta b_g^b & \delta c \end{bmatrix}^T,\ w:\ N(0,Q)$$
$$\delta p = \begin{bmatrix} \delta\phi & \delta\lambda & \delta h \end{bmatrix}^T, \delta v = \begin{bmatrix} \delta v_N & \delta v_E & \delta v_D \end{bmatrix}^T, \delta\varepsilon = \begin{bmatrix} \delta\varepsilon_N & \delta\varepsilon_E & \delta\varepsilon_D \end{bmatrix}^T$$
$$\delta b_a^b = \begin{bmatrix} \delta b_{ax}^b & \delta b_{ay}^b & \delta b_{az}^b \end{bmatrix}^T, \delta b_g^b = \begin{bmatrix} \delta b_{gx}^b & \delta b_{gy}^b & \delta b_{gz}^b \end{bmatrix}^T, \delta c = \begin{bmatrix} \delta B & \delta B \end{bmatrix}^T$$
$$F = \begin{bmatrix} F_{pp} & F_{pv} & 0_{3\times3} & 0_{3\times3} & 0_{3\times3} & 0_{3\times2} \\ F_{vp} & F_{vv} & F_{v\varepsilon} & F_{va} & 0_{3\times3} & 0_{3\times2} \\ F_{\varepsilon p} & F_{\varepsilon v} & F_{\varepsilon\varepsilon} & 0_{3\times3} & F_{\varepsilon g} & 0_{3\times2} \\ 0_{3\times3} & 0_{3\times3} & 0_{3\times3} & 0_{3\times3} & 0_{3\times3} & 0_{3\times2} \\ 0_{3\times3} & 0_{3\times3} & 0_{3\times3} & 0_{3\times3} & 0_{3\times3} & 0_{3\times2} \\ 0_{2\times3} & 0_{2\times3} & 0_{2\times3} & 0_{2\times3} & 0_{2\times3} & F_{cc} \end{bmatrix}, \Gamma = \begin{bmatrix} 0_{3\times3} & 0_{3\times3} & 0 \\ I_{3\times3} & 0_{3\times3} & 0 \\ 0_{3\times3} & I_{3\times3} & 0 \\ 0_{3\times3} & 0_{3\times3} & 0 \\ 0_{3\times3} & 0_{3\times3} & 0 \\ 0 & 0 & 0 \\ 0 & 0 & 1 \end{bmatrix}$$

In the above equation, δ represents the error, ϕ is the latitude, λ is the longitude, h is the altitude, v is the velocity, ε is the attitude, b_a^b is the accelerometer error, b_g^b is the gyroscope error, B is the GPS receiver clock error, and w is the process noise. F_{pp}, F_{pv}, F_{vp}, F_{vv}, $F_{v\varepsilon}$, F_{va}, $F_{\varepsilon p}$, $F_{\varepsilon v}$, $F_{\varepsilon\varepsilon}$, $F_{\varepsilon g}$, and F_{cc}, which are the components of matrix F, were defined by Titterton & Weston (2004). The pseudorange and Doppler measurement model of the GPS receiver can be expressed as

$$\delta z_{GPS} = H_{GPS}\delta x + v_{GPS} \tag{2}$$

where

$$\delta z_{GPS} = \begin{bmatrix} \delta z_\rho^1 & L & \delta z_\rho^m & \delta z_{\dot\rho}^1 & L & \delta z_{\dot\rho}^m \end{bmatrix}^T$$
$$\delta z_\rho^i = \rho_{INS}^i - \rho_{GPS}^i = -e_i^T M_l^e \delta p - \delta B + v_\rho^i$$
$$\delta z_{\dot\rho}^i = \dot\rho_{INS}^i - \dot\rho_{GPS}^i = -e_i^T M_n^e \delta v - \delta B + v_{\dot\rho}^i$$
$$H_{GPS} = \begin{bmatrix} -e_1^T M_l^e & 0_{1\times3} & 0_{1\times3} & 0_{1\times3} & 0_{1\times3} & -1 & 0 \\ M & M & M & M & M & M & M \\ -e_m^T M_l^e & 0_{1\times3} & 0_{1\times3} & 0_{1\times3} & 0_{1\times3} & -1 & 0 \\ 0_{1\times3} & -e_1^T M_n^e & 0_{1\times3} & 0_{1\times3} & 0_{1\times3} & 0 & -1 \\ M & M & M & M & M & M & M \\ 0_{1\times3} & -e_m^T M_n^e & 0_{1\times3} & 0_{1\times3} & 0_{1\times3} & 0 & -1 \end{bmatrix}$$
$$v_{GPS} = \begin{bmatrix} v_\rho^1 & L & v_\rho^m & v_{\dot\rho}^1 & L & v_{\dot\rho}^m \end{bmatrix}^T$$

In the above equation, ρ is the pseudorange measurement, $\dot\rho$ is the Doppler measurement, v_ρ and $v_{\dot\rho}$ are the noises of the GPS pseudorange and Doppler measurement, and e

https://doi.org/10.11003/JPNT.2018.7.3.155

is the line-of-sight vector. The coordinate transformation matrices M_l^e and M_n^e were defined by Titterton & Weston (2004). The extended Kalman filter based on the above model can prevent the divergence of the navigation solution and perform stable navigation by estimating the navigation solution error, inertial sensor error, and GPS receiver clock error.

As the GPS receiver provides information on the position and velocity of the user, it is possible to continuously observe the position and velocity errors under the normal operating conditions of GPS. However, observability analysis is required to examine whether it is possible to observe other state variables such as the attitude and inertial sensor error. According to the results of observability analysis, the GPS/INS integrated navigation system lacks observability for the attitude and the related inertial sensor error in a static state (Bar-Itzhack & Berman 1988). If a UAV flies a trajectory requiring acceleration, observability is improved (Bar-Itzhack & Porat 1980, Porat & Bar-Itzhack 1981). However, as it maintains a static cruise state for most of the time while heading toward a destination for mission accomplishment, it is necessary to address such observability problems. In particular, when low-cost inertial sensors are used, it is difficult to obtain the attitude information through the measurement of the rotational speed of the earth. Therefore, the integration of the magnetometer has been widely used to supplement the observability for the attitude information.

Under the normal operating condition of GPS, it is possible to obtain stable navigation performance because error state variables can be continuously estimated using GPS measurements, and observability for the attitude error can be obtained through the integration of the magnetometer. However, GPS may fail owing to external factors, such as jamming. In this case, navigation is performed using only the inertial sensor without GPS and the navigation solution diverges owing to the accumulation of the inertial sensor errors. As the divergence speed of the navigation solution depends on the estimation accuracy of the attitude and inertial sensor errors, it is necessary to improve observability to enhance the estimation accuracy. Subsequently, the magnetic heading aiding method and vector aiding method, which are the integration methods of the magnetometer, are introduced and compared. The advantages of the proposed magnetic vector aiding method over the magnetic heading aiding method, which has been widely used, are analyzed, and the performance enhancement of the GPS/INS integrated navigation system using the proposed method is described.

3. MAGNETOMETER AIDING METHODS

3.1 Magnetic Heading Aiding Method

The magnetic north pole of the earth is different from the actual North Pole, and the distribution of the geomagnetic field is not uniform but varies depending on the region in a complicated manner. For such a distribution of the geomagnetic field, models such as the World Magnetic Model (Maus et al. 2010) and International Geomagnetic Reference Field (Finlay et al. 2010) have been provided, and the magnetic heading aiding method has been widely used to obtain the attitude information from the geomagnetic field. This method can measure the heading using the magnetic vector measured with the magnetometer installed in a flight vehicle based on the body frame and the declination provided by the geomagnetic field model (Gebre-Egziabher 2004). The equation for magnetic heading measurement is

$$\delta z_\Psi = \Psi_{INS} - \Psi_m = H_\Psi \delta x + v_\Psi \tag{3}$$

where

$$\Psi_m = -\arctan\left(\frac{h_Y^l}{h_X^l}\right) + \delta_m$$
$$h_X^l = h_X^b \cos\theta + h_Y^b \sin\phi \sin\theta + h_Z^b \cos\phi \sin\theta$$
$$h_Y^l = h_Y^b \cos\phi - h_Z^b \sin\phi$$
$$H_\Psi = \begin{bmatrix} 0_{1\times3} & 0_{1\times3} & 0 & 0 & 1 & 0_{1\times3} & 0_{1\times3} & 0_{1\times2} \end{bmatrix}$$

In the above equation, Ψ_m is the heading calculated from the measured geomagnetic field, v_Ψ is the noise of the magnetic heading measurement, δ_m is the declination representing the difference between the magnetic north pole and the actual North Pole, h_X^b, h_Y^b and h_Z^b are the components of the magnetic vector measured using the magnetometer, and ϕ and θ are the roll and pitch angles of the flight vehicle, respectively. As shown in Eq. (3), the roll and pitch angles affect the heading as they are used in the calculation of the heading. However, they are usually omitted from the measurement equation because they can be assumed to be small under the normal operating conditions of GPS.

The magnetic heading aiding method is a method of calculating the heading using only the horizontal component of the geomagnetic field as shown in Fig. 1. It is used to supplement the observability of heading of GPS/INS navigation systems. For GPS/INS navigations systems, however, the attitude diverges owing to the accumulation of the inertial sensor errors in the case of GPS failure. As the attitude information is required in the calculation process of the heading as shown in Eq. (3), the heading calculated

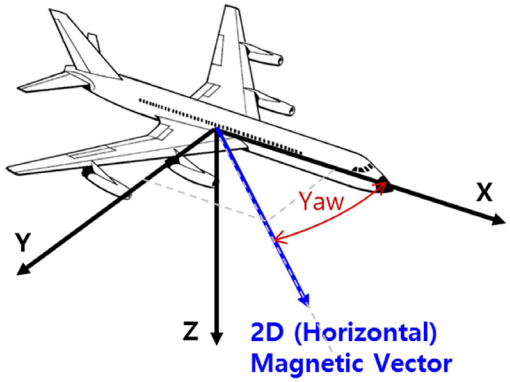

Fig. 1. Yaw angle information from magnetic heading aiding method. Magnetic heading aiding method provides only yaw angle information to the navigation system.

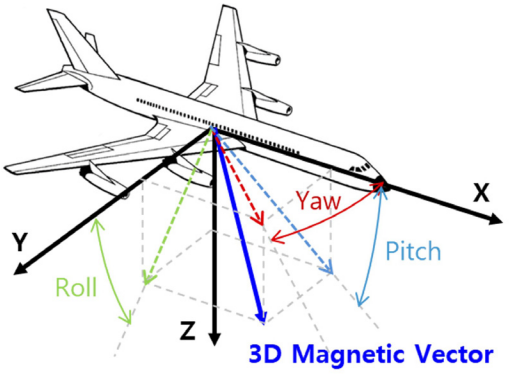

Fig. 2. Attitude information from magnetic vector aiding method. Magnetic vector aiding method provides information of all Euler angle to the navigation system.

using the diverging attitude also contains errors. Therefore, it is necessary to exercise caution when the magnetic heading aiding method is used in the case of GPS failure.

3.2 Magnetic Vector Aiding Method

The geomagnetic field has a 3D vector shape. As the roll and pitch angles can be determined using the gravity vector measured with the accelerometer, the attitude information of the two axes perpendicular to the vector direction can be obtained using the magnetic vector. If the magnetic vector of the body frame measured with the magnetometer is converted into the navigation frame using the attitude information of the navigation system and thereafter compared with the magnetic vector of the navigation frame obtained from the geomagnetic field model, the information on the attitude error can be obtained. The measurement equation for the magnetic vector based on this principle (Gebre-Egziabher & Elkaim 2008, Barczyk & Lynch 2012) is

$$\delta z_h = \begin{pmatrix} \delta h_N^n \\ \delta h_E^n \\ \delta h_D^n \end{pmatrix} = H_h \delta x + v_h \tag{4}$$

where

$$H_h = \begin{bmatrix} 0_{3\times3} & 0_{3\times3} & \begin{bmatrix} 0 & -h_D^n & h_E^n \\ h_D^n & 0 & -h_N^n \\ -h_E^n & h_N^n & 0 \end{bmatrix} & 0_{3\times3} & 0_{3\times3} & 0_{3\times2} \end{bmatrix}, v_h = C_{INS} \begin{pmatrix} v_{h,X} \\ v_{h,Y} \\ v_{h,Z} \end{pmatrix}$$

$$\begin{pmatrix} \delta h_N^n \\ \delta h_E^n \\ \delta h_D^n \end{pmatrix} = C_{INS} \cdot \begin{pmatrix} h_X^b \\ h_Y^b \\ h_Z^b \end{pmatrix} - \begin{pmatrix} h_N^n \\ h_E^n \\ h_D^n \end{pmatrix} = \begin{bmatrix} 0 & -h_D^n & h_E^n \\ h_D^n & 0 & -h_N^n \\ -h_E^n & h_N^n & 0 \end{bmatrix} \begin{pmatrix} \delta\varepsilon_N \\ \delta\varepsilon_E \\ \delta\varepsilon_D \end{pmatrix} + C_{INS} \begin{pmatrix} v_{h,X} \\ v_{h,Y} \\ v_{h,Z} \end{pmatrix}$$

In the above equation, δh_N^n, δh_E^n and δh_D^n are the error of the measured magnetic vector components when the magnetic vector measurements of the magnetometer are converted from the body frame to the navigation frame, C_{INS} is the direction cosine matrix including the attitude error of INS, $v_{h,X}$, $v_{h,Y}$ and $v_{h,Z}$ are the noises of the magnetic vector measurement components, and h_N^n, h_E^n and h_D^n are the components of the geomagnetic vector obtained from the model.

The magnetic vector has the information on not only the heading but also all three axes, as shown in Fig. 2. As shown in Eq. (4), the attitude error can be determined by comparing the magnetic vector measurement with the geomagnetic vector of the model. While the magnetic heading measurement matrix H_Ψ of Eq. (3) can observe only the heading error because it has a single row and thus, Rank(H_Ψ) = 1 , the magnetic vector measurement matrix H_h of Eq. (4) can provide improved observability because it has a skew-symmetric shape and thus, Rank(H_Ψ) = 2 is always true.

The attitude error of GPS/INS navigation systems is closely associated with the inertial sensor error estimation performance (Rhee et al. 2004). Therefore, if the attitude estimation accuracy is improved through the magnetic vector aiding method, it is possible to enhance the inertial sensor error estimation performance (No & Kee 2017). Moreover, as the attitude information is not necessary in the integration process unlike the heading aiding method, magnetic vector measurements can be utilized even in the case of GPS failure. The magnetic field, however, is easily affected by external factors such as nearby metal materials and electric current. Therefore, to successfully perform magnetic vector aiding, appropriate corrections and compensations for such external factors must be performed first.

4. SIMULATION

https://doi.org/10.11003/JPNT.2018.7.3.155

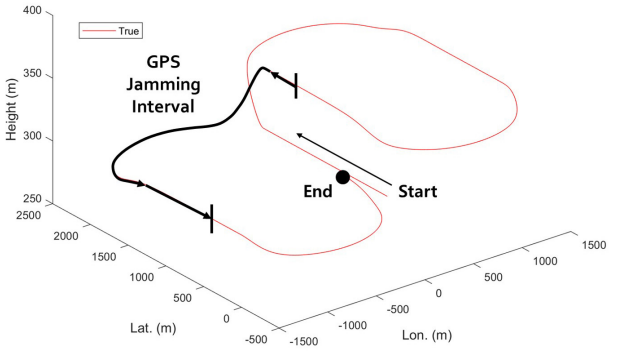

Fig. 3. Generated trajectory of aircraft in simulation. Aircraft performs several longitudinal and lateral maneuvers during the simulation. There is a 60 seconds interval of GPS jamming in case of simulation for jammed GPS condition.

4.1 Simulation Setup

To compare the performance of the proposed magnetic vector aiding method with that of the existing magnetic heading aiding method, simulations were performed using MATLAB. The inertial sensor, GPS pseudorange and Doppler measurements, and magnetometer data were generated by creating true values using the 6-degree-of-freedom aircraft motion equation and Navion aircraft (Teper 1969) model and thereafter inserting errors. The created trajectory of the aircraft is shown in Fig. 3.

Errors corresponding to low-cost sensors were inserted to the inertial sensor, GPS, and magnetometer measurement data. These measurements were processed with the aforementioned 17th order tightly coupled GPS/INS integrated navigation algorithm. Table 1 shows the detailed specifications of the generated sensor data. It was assumed that only noise existed in the magnetometer measurement under the premise that all errors caused by external metals and electric current were eliminated through appropriate corrections. To simulate a GPS failure, the use of all GPS measurements was stopped for 60 s in the 140-200 s interval marked in Fig. 3. After 200 s, GPS measurements were normally used again.

4.2 Simulation Result for Normal GPS Condition

To examine the performance change caused by the observability difference according to the integration method of the magnetometer, simulation was performed for normal GPS conditions. Tables 2 and 3 and Figs. 4-7 show the position results and velocity, attitude, and accelerometer error estimation results of the three navigation methods under normal GPS condition. In terms of the position and velocity, all three navigation methods exhibited similar

Table 1. Sensor output-rate and error specification.

Sensor	Output-rate (Hz)	Error specification
Gyroscope	100	Initial bias: 3 deg/s (1σ) Time-varying bias: 1st order Gauss-Markov model rate random walk (RRW): 0.007 deg/s time constant: 300 sec Noise: random walk (RW) 2 deg/$\sqrt{\text{hr}}$
Accelerometer	100	Initial bias: 8 mg (1σ) Time-varying bias: 1st order Gauss-Markov model rate random walk (RRW): 0.1 mg time constant: 300 sec Noise: random walk (RW) 0.12 m/s/$\sqrt{\text{hr}}$
GPS	4	Pseudorange noise: Exponential model (1σ 0.22 m at El 20 deg) Doppler noise: Exponential model (1σ 0.042 m/s at El 20 deg)
Magnetometer	100	Noise: 1σ 5 mgauss

Table 2. Position and velocity RMS error results in normal GPS condition.

	Pos. N (m)	Pos. E (m)	Pos. D (m)	Vel. N (m/s)	Vel. E (m/s)	Vel. D (m/s)
GPS/INS	0.18	0.13	0.22	0.022	0.015	0.016
GPS/INS/w Heading	0.18	0.13	0.22	0.021	0.015	0.016
GPS/INS/w Vector	0.18	0.13	0.22	0.019	0.014	0.016

accuracy. This is because the information of position and velocity is directly provided by GPS measurements and are thus highly dependent on GPS measurements. In terms of the velocity, however, the results of the magnetic vector aiding were slightly improved. This was caused by the improvement of the attitude and accelerometer error estimation performance to be mentioned later.

The attitude accuracy showed the largest differences in the results of the three navigation methods. The results of the GPS/INS navigation method without the use of the magnetometer showed large errors in the initial 30 s interval of Fig. 6 owing to the insufficient observability for the heading. This was caused by the unique characteristics of the low-cost GPS/INS system, which lacked observability for the heading when the flight vehicle did not accelerate in the horizontal direction. It was confirmed that such heading errors affected not only the initial interval but also the accuracy of the roll and pitch angles in the 30-120 s interval. As for the results of the magnetic heading aiding, the heading performance was improved by approximately 58% from 0.64° to 0.27° because the heading observability of the low-cost GPS/INS navigation system was enhanced. This also improved the performance degradation of the roll and pitch angles in the 30-120 s interval. As for the magnetic vector aiding method, the attitude performances of all axes were enhanced because the observability was enhanced. Therefore, the roll angle, pitch angle, and heading were improved by 61%, 50%, and 56%, respectively, compared with those for the magnetic heading

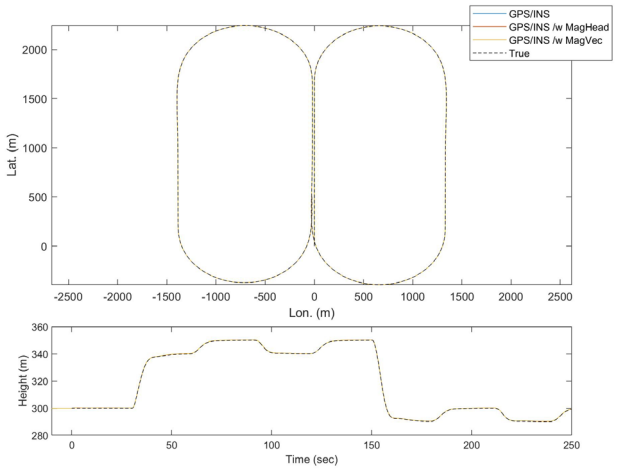

Fig. 4. Position results in normal GPS condition. All methods show identical position performance because the position mostly depends on GPS measurements.

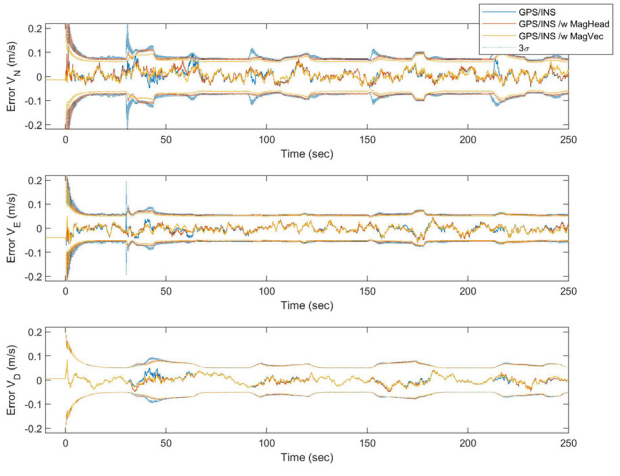

Fig. 5. Velocity results in normal GPS condition. Magnetic vector aiding method shows slightly better performance due to its enhanced attitude and sensor error estimation.

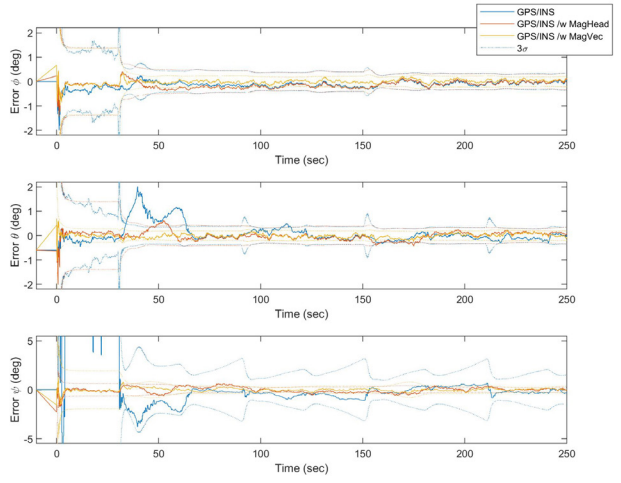

Fig. 6. Attitude results in normal GPS condition. Magnetic heading aiding method enhances yaw angle accuracy. Magnetic vector improves all Euler angle accuracy due to its higher observability.

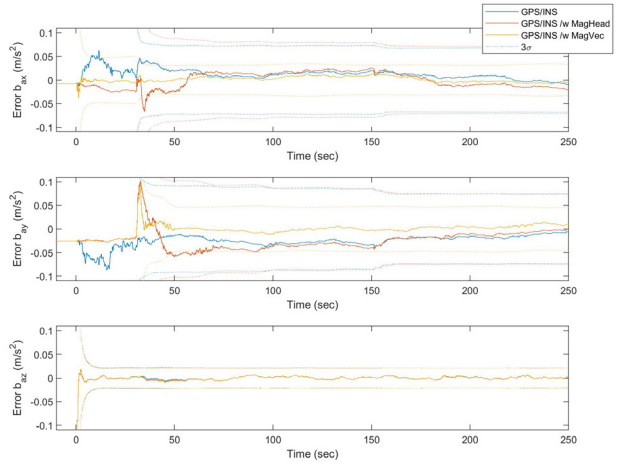

Fig. 7. Accelerometer bias results in normal GPS condition. Magnetic vector aiding method estimates accelerometer bias error more accurately due to its enhanced observability for attitude and sensor error.

aiding method.

Table 3 and Fig. 7 show the results of the estimation of the accelerometer error for the three navigation methods under normal GPS conditions. Owing to the aforementioned relationship between the attitude error and the inertial sensor error estimation performance, the accelerometer error estimation accuracy of the magnetic vector aiding method improved by 50% for the X-axis and 78% for the Y-axis compared with that of the existing GPS/INS navigation method. As for the results of the accelerometer error estimation for the Z-axis, all three navigation methods exhibited similar results because they had high observability already. In the case of the magnetic heading aiding method, however, the accelerometer error estimation accuracy for the X-axis and Y-axis was lower compared with that of the existing GPS/INS navigation method. This appears to be because the magnetic heading error model omitted the attitude error even though it was affected by the roll and pitch angles, and this modeling error affected the convergence of the accelerometer error estimation values in the 30–60 s interval in which the roll and pitch angles were unstable.

Table 3. Attitude and accelerometer bias RMS error results in normal GPS condition.

	Roll (deg)	Pitch (deg)	Yaw (deg)	b_{ax} (m/s^2)	b_{ay} (m/s^2)	b_{az} (m/s^2)
GPS/INS	0.14	0.28	0.64	0.012	0.023	0.003
GPS/INS/w Heading	0.18	0.16	0.27	0.015	0.031	0.003
GPS/INS/w Vector	0.07	0.08	0.12	0.006	0.005	0.003

In summary, in the simulation with normal GPS conditions, the magnetic vector aiding method exhibited

Table 4. Position and velocity error after 60 sec of GPS jamming.

	Pos. N (m)	Pos. E (m)	Pos. D (m)	Vel. N (m/s)	Vel. E (m/s)	Vel. D (m/s)
GPS/INS	44.8	188.6	30.5	0.792	-8.513	-1.557
GPS/INS/w Heading	1793.2	2463.4	1124.7	8.947	-147.4	-45.57
GPS/INS/w Vector	9.8	77.9	4.3	-0.024	-3.518	-0.452

Table 5. Attitude error after 60 sec of GPS jamming.

	Roll (deg)	Pitch (deg)	Yaw (deg)
GPS/INS	1.66	0.59	3.42
GPS/INS/w Heading	57.44	26.57	42.64
GPS/INS/w Vector	0.80	0.12	1.25

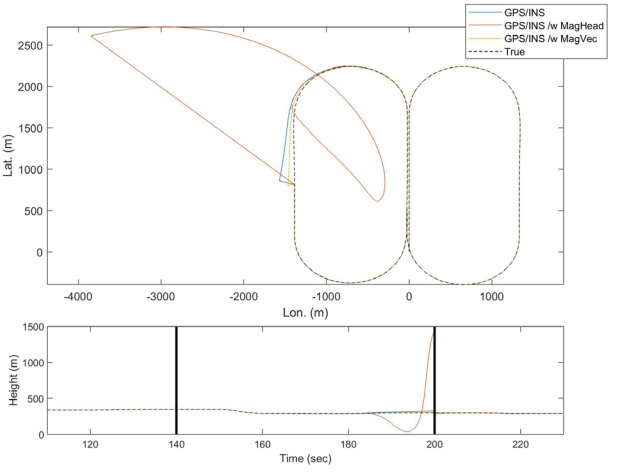

Fig. 8. Position results in jammed GPS condition. Magnetic heading aiding method shows huge error due to its erroneous heading information update. Magnetic vector aiding method reduces position divergence because it provides correct attitude information even if GPS is not working.

improved velocity, attitude, and accelerometer error estimation performance. This simulation result suggests that the proposed method will suppress the divergence of the navigation solution in the case of GPS failure.

4.3 Simulation Result for Jammed GPS Condition

The magnetic vector aiding method has two advantages over the existing magnetic heading aiding method. First, it provides improved attitude observability compared with the magnetic heading aiding method, which uses only 2D plane information, because it utilizes all information of the 3D magnetic vector. Therefore, it is possible to improve the estimation performance for the attitude and inertial sensor error–in particular, the accelerometer error (No & Kee 2017). Second, the magnetic vector aiding method can continuously provide proper attitude information even in case of GPS failure because it performs integration without attitude information whereas the heading aiding method requires attitude information from the navigation system.

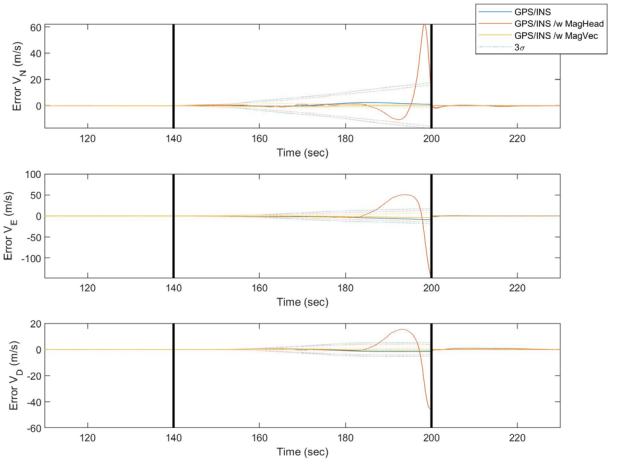

Fig. 9. Velocity results in jammed GPS condition. Magnetic heading aiding method shows erroneous results. Magnetic vector aiding method reduces divergence of velocity.

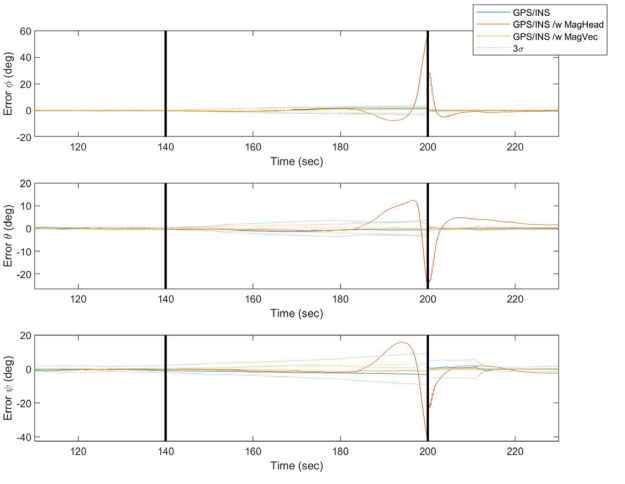

Fig. 10. Attitude results in jammed GPS condition. Magnetic heading aiding method shows erroneous results even in yaw angle. Magnetic vector aiding method maintains small attitude error compared to other methods.

These two advantages are important characteristics that can suppress the divergence of the navigation solution in case of GPS failure. To confirm these advantages, simulation was performed for the GPS failure situation.

Tables 4 and 5 show the position, velocity, and attitude error results after the use of GPS was stopped for 60 s. Figs. 8-10 are graphs showing the position, velocity, and attitude results under the GPS failure situation. Above all, the magnetic heading aiding method showed several times to several tens of times larger errors than the other methods in terms of the position, velocity, and attitude. This was because the inertial sensor errors were accumulated to the roll and pitch angles from the moment at which GPS could not be used and the magnetic heading aiding method using

these angles provided inaccurate heading information. Such inaccurate heading information further accelerated the divergence of the error of the navigation solution, indicating that it is desirable to stop using the magnetic heading aiding method in case GPS cannot be used.

The magnetic vector aiding method delayed the divergence of the attitude error of the navigation system as shown in Fig. 10, thereby reducing the roll angle, pitch angle, and heading errors at 60 s after GPS failure by 52%, 80%, and 63%, respectively. It also decreased the position errors in the north, east, and vertical directions at 60 s after GPS failure by 78%, 59%, and 86%, respectively, by delaying the divergence of the velocity and position errors. These effects could be obtained because the magnetic vector aiding method can provide proper attitude information even in the case of GPS failure and its improved observability enables the estimation of more accurate inertial sensor errors.

Thus, two contradictory results–degradation or improvement of the navigation performance–could be obtained depending on the method of application of the three–axis magnetometer to navigation systems, i.e., heading or vector aiding.

5. CONCLUSIONS

This study proposed a method of responding to GPS failure by integrating 3D magnetic vector measurements with the GPS/INS navigation system. It is necessary to exercise caution when using the existing magnetic heading aiding method because it may degrade the navigation performance in case of GPS failure even though it is useful for supplementing the observability of low-cost GPS/INS navigation systems for the heading. The magnetic vector aiding method provides improved observability compared with the magnetic heading aiding method, thus enabling more accurate estimation of attitude and inertial sensor errors. It can also continuously provide accurate attitude information even when the attitude error increases owing to GPS failure because it does not require attitude information in the integration process. Although the use of the proposed magnetic vector aiding method cannot prevent the divergence of the navigation solution in the case of GPS failure, it can enhance the stability of the navigation system by reducing the divergence speed of the navigation solution owing to the aforementioned advantages.

The simulation results confirmed that the magnetic vector aiding method improved the attitude accuracy and the sensor error estimation accuracy, thereby reducing the divergence speed of the navigation error in the case of GPS failure. The proposed method has significant implications because it can enhance the stability of UAVs in the case of GPS failure without additional cost through the improved integration method for the measurements of the existing magnetometer.

ACKNOWLEDGMENTS

This research was supported by the Lockheed Martin Corporation through the Republic of Korea Science and Technology (RoKST&R) Program, contracted through the Institute of Advanced Aerospace Technology at Seoul National University.

REFERENCES

Bar-Itzhack, I. Y. & Berman, N. 1988, Control theoretic approach to inertial navigation systems, Journal of Guidance, Control, and Dynamics, 11, 237-245. https://doi.org/10.2514/3.20299

Bar-Itzhack, I. Y. & Porat, B. 1980, Azimuth observability enhancement during inertial navigation system in-flight alignment, Journal of Guidance, Control, and Dynamics, 3, 337-344. https://doi.org/10.2514/3.55999

Barczyk, M. & Lynch, A. F. 2012, Integration of a Triaxial Magnetometer into a Helicopter UAV GPS-Aided INS, IEEE Transactions on Aerospace and Electronic Systems, 48, 2947-2960. https://doi.org/10.1109/TAES.2012.6324671

Finlay, C. C., Maus, S., Beggan, C. D., Bondar, T. N., Chambodut, A., et al. 2010, International geomagnetic reference field: the eleventh generation, Geophysical Journal International, 183, 1216-1230. https://doi.org/10.1111/j.1365-246X.2010.04804.x

Gebre-Egziabher, D. 2004, Design and performance analysis of a low-cost aided dead reckoning navigator, PhD Dissertation, Stanford University.

Gebre-Egziabher, D. & Elkaim, G. H. 2008, MAV attitude determination by vector matching, IEEE Transactions on Aerospace and Electronic Systems, 44, 1012-1028. https://doi.org/10.1109/TAES.2008.4655360

Maus, S., Macmillan, S., McLean, S., Hamilton, B., Nair, M., et al. 2010, The US/UK world magnetic model for 2010-2015, NOAA Technical Report NESDIS/NGDC.

No, H. & Kee, C. 2017, Observability Enhancement of a GPS/INS Navigation System Using a Triaxial Magnetometer, Transactions of the Japan Society for Aeronautical and Space Sciences, submitted.

Porat, B. & Bar-Itzhack, I. Y. 1981, Effect of acceleration

switching during INS in-flight alignment, Journal of Guidance and Control, 4, 385-389. https://doi.org/10.2514/3.19744

Rhee, I., Abdel-Hafez, M. F., & Speyer, J. L. 2004, Observability of an integrated GPS/INS during maneuvers, IEEE Transactions on Aerospace and Electronic Systems, 40, 526-535. https://doi.org/10.1109/TAES.2004.1310002

Teper, G. L. 1969, Aircraft stability and control data, NASA Ames Research Center Technical Report, NASA/CR-96008.

Titterton, D. & Weston, J. L. 2004, Strapdown inertial navigation technology, 2nd ed. (London: The Institution of Engineering and Technology)

Heekwon No is a postdoctoral researcher in the School of Mechanical and Aerospace Engineering at Seoul National University. He received B.S. and Ph.D. degrees from the same university. His research interests are the cost effective attitude determination, navigation, guidance and automatic control system of the unmanned aerial vehicle.

Junesol Song is a postdoctoral researcher in the School of Mechanical and Aerospace Engineering at Seoul National University. She received B.S. and Ph.D. degrees from the same university. Her research interests include carrier phase based algorithms and positioning.

Jungbeom Kim is a Ph.D. candidate of GNSS Lab. in the School of Mechanical and Aerospace Engineering at Seoul National University. He received the B.S and Master degree from Seoul National University. His recent research interests DGPS, FKP and Improvement of L1 single frequency GPS receiver's positioning accuracy.

Yonghwan Bae is a M.S. student of GNSS Lab. in the School of Mechanical and Aerospace Engineering at Seoul National University, South Korea. He received the B.S. from Seoul National University. His research interests include the unmanned aerial vehicle and cube-satellite.

Changdon Kee is a Professor in the School of Mechanical and Aerospace Engineering at Seoul National University (SNU), South Korea and supervises SNU GNSS Lab (SNUGL, http://gnss.snu.ac.kr). He received B.S. and M.S. degrees from Seoul National University and a Ph.D. degree from Stanford University. He served as a Technical Advisor to the Federal Aviation Administration (FAA) on the Wide Area Augmentation System (WAAS) in 1994. Prof. Kee currently serves as a Technical Advisor for Korea Civil Aviation Safety Authority (KCASA) and Ministry of Public Administration and Security (MOPAS). He also serves as a Vice President of Korean Institute of Navigation. He has more than 20 years of GNSS and flight control research experiences.